*Journal of Metals, Materials and Minerals, Vol.27 No.1 pp.39-45, 2017*

# Antireflective Surface of Nanostructures Fabricated by $CF_4$ Plasma Etching

**Witchaphol SOMRANG[1], Somyod DENCHITCHAROEN[1,*], Pitak EIAMCHAI[2], Mati HORPRATHUM[2] and Chanunthorn CHANANONNAWATHORN[2]**

*[1]Department of Physics, King Mongkut's University of Technology Thonburi, 126 Pracha Uthit Rd.,Thung Khru, Bangkok 10140, Thailand*

*[2]National Electronics and Computer Technology Center, 112 Thailand Science Park, Phahonyothin Rd., Klong 1,Klong Luang, Pathumthani 12120, Thailand*

## Abstract

In this research, the nanostructures surface was fabricated by the $CF_4$ plasma etching process on the $SiO_2$-based substrates for antireflection applications. The nickel films were firstly deposited on the substrates by the sputtering system. The prepared Ni layers were then annealed at 500°C for 1 min in order to promote dewetting process to be used as metal masks. During the etching process, $CF_4$ etching condition was performed for 15-60 min. to create the $SiO_2$ nanopillars. After the etching process, the samples were immersed in nitric acid for 5 min. to remove the nickel masks. The $SiO_2$ nanopillars without Ni were investigated for physical morphologies and optical properties by the field-emission scanning electron microscopy (FESEM) and UV-Vis-NIR spectroscopy respectively. The results showed that the etching conditions greatly affected the sizes and shapes of the nanostructures, as well as improved the antireflection properties of the $SiO_2$ based materials.

**Keywords**: Antireflection; Dewetting; Plasma etching.

## Introduction

The antireflection properties of surfaces have been widely studied about improving the performance of optical devices such as display panels for electronic solar cells and optical sensors.[1-9] Generally, however, most optical devices suffer from high surface reflection which degrades the performance of the optical system. The Antireflection (AR) coatings are therefore required to eliminate undesired optical loss whereas the transmission through optical element is higher. In the recent years, the single-layer or multilayer antireflection coating was an approach to reduce the optical reflection.[10-12] However, this technique has limitation with thermal expansion mismatch, selection of suitable materials and instability of thin film stacks.[3, 5, 13] In order to avoid the aforementioned problems from light reflection, many approaches have been introduced such as fabrications of sub-wavelength structures instead of the AR coatings. These sub-wavelength structures could improve the undesired surface reflection, from which the conventional AR coatings suffer.[14-15] Various methods to fabricate the AR surface of the nanostructures include nanoimprint lithography, laser interference lithography, and electron beam lithography. However, all of these methods require costly and complicated of fabrication procedures.[13, 16-17]

In this work, we reported a fabrication technique which was a simple, high-throughput, and cost-effective method. We proposed the fabrication of the AR surface based on randomly distributed Ni nanoparticles on $SiO_2$ substrates. A plasma reactor with $CF_4$ gas was used to transfer pattern of nanorods on $SiO_2$-based substrates, which are widely used for optical and electronic applications.[18-20] In addition, the average size and shape dependent optical properties of nanostructures were also studied.

## Materials and Experimental Procedure

### *Preparation of $SiO_2$/Si substrate*

The $SiO_2$ films with a thickness of 1 μm on Si (100) substrates were cleaned by acetone and isopropyl alcohol in an ultrasonic bath for 45 min. The substrates were further cleaned by plasma treatment in order to eliminate impurities and contaminants from surfaces by sputtering technique.

* Corresponding author. E-mail: led_material@hotmail.com

*DOI: 10.14456/jmmm.2017.6*

*Fabrication of nanostructured $SiO_2$ surfaces*

The antireflective nanostructured $SiO_2$ surfaces were prepared by two main steps such as thermal annealing and reactive ion etching process. The 1 μm $SiO_2$/Si substrates were deposited nickel thin films by DC magnetron sputtering with deposition times for 60 and 90 s. The rapid thermal annealing was subsequently introduced to agglomerate nickel at 500°C for 1 min. to form nanoparticles array. These nickel nanoparticles were acted as a mask for reactive ion etching process. The patterned substrates were subsequently etched using CF4 plasma with an etching duration from 15 to 60 min by plasma-enhanced chemical vapor deposition (PE-CVD). The gas pressure were maintained at $6\times10^{-3}$ mbar and RF power of 200 W for 15, 30, 45 and 60 min. respectively. The nanodot patterns were transferred to a part of $SiO_2$ layer to be $SiO_2$ nano-columns. After plasma etching, residual Ni on top of $SiO_2$ was removed using nitric acid ($HNO_3$) for 5 min.

*Characterization*

The morphologies of both nano-pattern mask and $SiO_2$ nanostructure were observed by field-emission scanning electron microscopy (FE-SEM, HITACHI SU8030). The optical reflectance was examined by a UV-Vis-NIR spectrophotometry (Agilent Cary 7000 Universal Measurement Spectrophotometer) in the region of 200-2,000 nm. All the reflectance spectra were collected from an incident angle of light source to the substrate normal at 8.

## Results and Discussion

*Characterization of the surface morphology*

The Figure 1 shows the field-emission scanning electron microscopy images of the Ni nanoparticles after annealing for 1 min. at 500°C. When heated at such temperature, the very thin film of Ni would agglomerate to form arrays of nanoparticles and covered the entire surface of each substrates due to increased surface energy. The average diameter and density of Ni nanoparticles depended on the thickness of Ni thin film and the annealing temperature.[21-22] From the figures, different sizes of randomly arranged nanostructures on $SiO_2$/Si substrates were shown. The Ni nanoparticles prepared at different deposition time exhibited different average sizes in the diameter. We calculated the average diameter and density of randomly distributed Ni nanoparticles in the SEM images

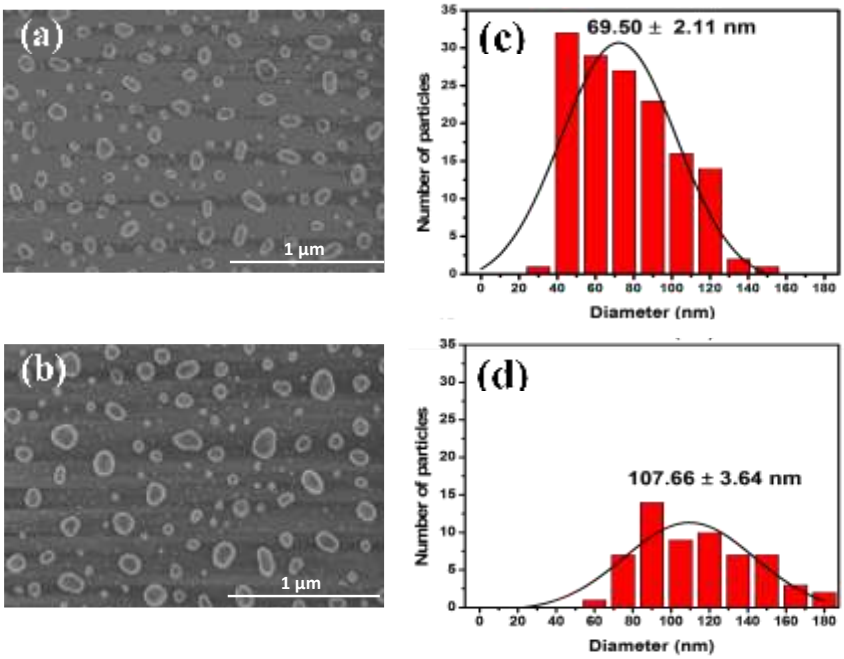


**Figure 1.** Surface morphologies and diameter distribution of Ni particles on $SiO_2$/Si substrate with Ni deposition times of (a) 60 s. (b) 90 sec. after annealed at 500°C for 1 min. and (c, d) corresponding diameter distribution of Ni nanoparticles

The average sizes of the nanoscale structures with deposition times of 60 and 90 s were estimated by 69.50 ± 2.11 nm and 107.66 ± 3.64 nm, respectively. As a result, the increase in the deposition time corresponded to the increased various thickness of the Ni film. Therefore, Ni film was completely dewetted after the annealing treatments, and resulted in the increase of the average particle in diameter.[23-24] In addition, the determined density of the nanoparticles with Ni deposition times of 60 and 90 s. were 32.25 and 23.80 g/cm$^3$, respectively.

From Figure 1(a), the 60 s Ni thin film was separated into nanoparticulates on the substrate surface. As expected, we observed that the average diameter of Ni nanoparticles was much smaller than the nanoparticles that change from the 90 s. Ni thin film in the Figure 1(b). The Ni nanoparticles were larger in size because of the longer Ni deposition time. The larger size and inter-nanoparticle distance were thought to allow the improved etching process. We expected that the larger size of the Ni nanoparticles would be able to properly mask the substrates during the plasma etching proces

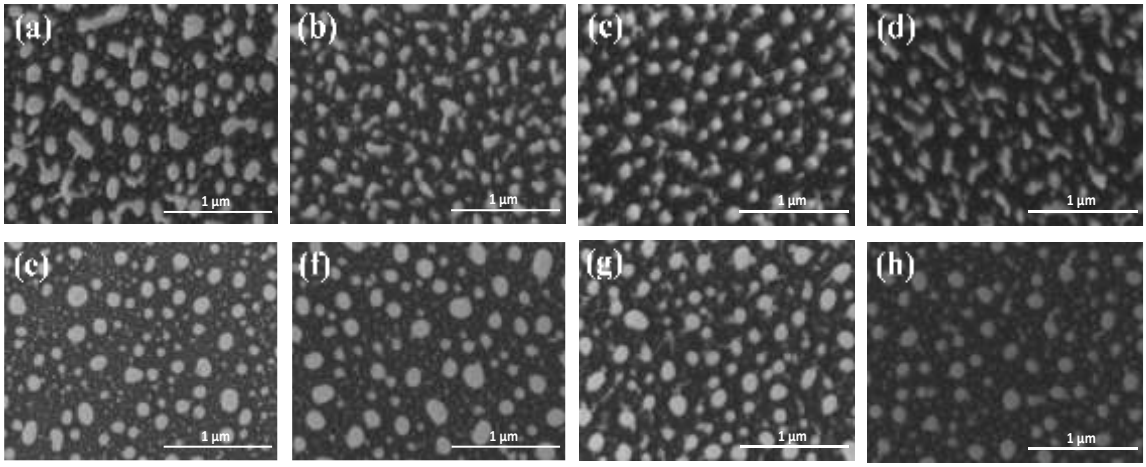


**Figure 2.** Top-view: SEM images of nanostructured $SiO_2$ surfaces after etched for (a) 15 min. (b) 30 min. (c) 45 min. (d) 60 min. (Ni deposition time for 60 s.) (e) 15 min. (f) 30 min. (g) 45 min. and (h) 60 min. (Ni deposition time for 90 s.).

Figure 2 shows the top view of nanostructured $SiO_2$ surfaces. In case of Ni deposition time for 60 s, immediately after the etching process of the samples for 15 min. from Figure 2(a). We observed that drastically changes in morphologies of the nanoparticles in comparison to those of the Ni masks from before the etching. When the plasma etching time was increased, the diameter of nanostructure was slightly distorted from Figure 2(b) and 2(c). Further increase in the etching time to 60 min., as shown in Figure 2(d), clearly yielded the nanostructures which were obviously deformed. While Ni deposition time for 90 s were also nearly well-defined and not changing of nanopillar diameter. Figure 2(h), the morphology of diameter and shape were changed noticeably because of the Ni Mask can also etched by reactive ions of $CF_4$ gas.

From morphology of nanostructured $SiO_2$ surfaces as shown in Figure 2, the diameter, density and periodicity of the mask patterns can be estimated. The Figure 3 shows the average diameter, density and average period of nanopatterns as a function of etching time in plasma etching process. The average diameter of nanoparticles and the average period between adjacent nanoparticulates were increased whereas the density was decreased as the plasma duration was increased.[4, 25] The Figure 3(a) in case of Ni deposition time for 60 s (red line), the average diameters were increased from 124.18 ± 3.54 nm at etching time 15 min. to 129.33 ± 3.46 nm at etching time 60 min. In case of deposition time for 90 s (blue line), the average diameters were increased from 117.57 ± 3.48 nm at etching time 15 min. to 121.18 ± 2.95 nm at etching time 60 min.

From the Figure 3(b) in case of Ni deposition time for 60 sec. (red line) and 90 s (blue line), the density of Ni nanoparticles was decreased to 20.66 and 16.17 g/cm$^3$, respectively when the etching time was increased to 60 min. Whereas, the average period was increased to 278.08 ± 7.39 nm for Ni deposition time for 60 s (red line) and 295.36 ± 5.38 nm for deposition time for 90 s (blue line) as shown in the Figure 3(c). However, the measured value of nanostructured $SiO_2$ surfaces (Ni deposition time for 60 s) was slightly fluctuated due to variation from randomly

.arranged on the substrates after etching time. Therefore the average size, density and period of nanostructured $SiO_2$ surfaces can be controlled by the plasma duration.

The $SiO_2$ surfaces with the Ni nanoparticles, prepared at 60 and 90 sec. and annealed at 500°C for 1 min., were then etched with the $CF_4$ plasma for the different lengths of time, as shown in Figure 4. From the figures, we observed that the Ni masks successfully resisted the continuous plasma etching whereas the regions without Ni mask were etched rapidly. The etching process therefore caused the surface to evolve into the nanopillar shape.

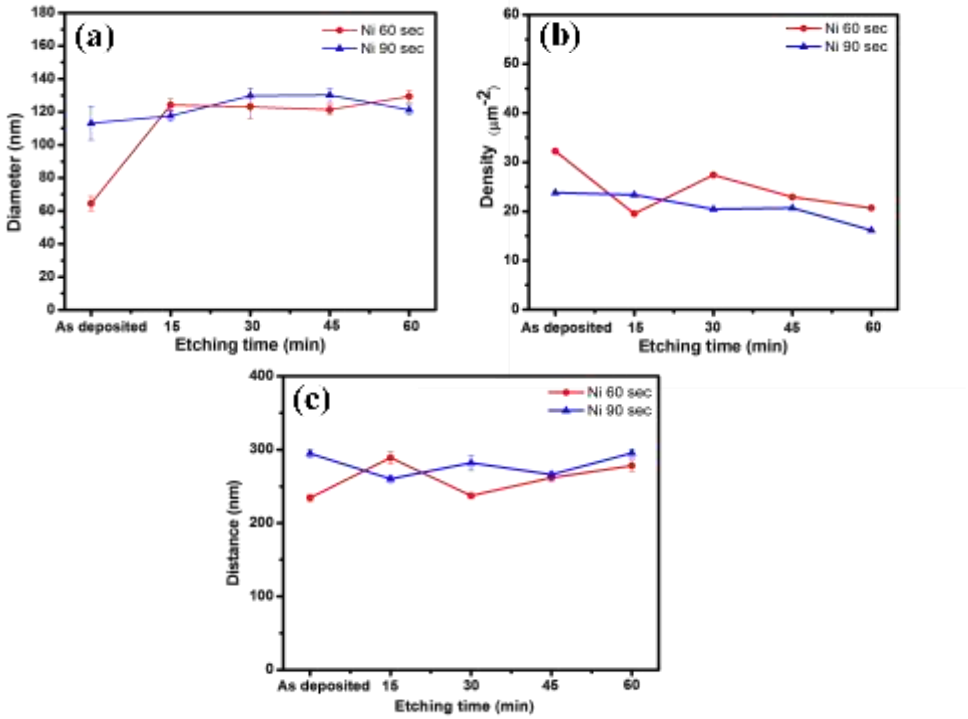


**Figure 3.** (a) The average diameter, (b) density and (c) average period of nanopatterns as a function of etching time in CF4 plasma etching process for 15-60 min.

From the SEM images in the Figure 4(a)-4(d), the heights of the nanostructures were controlled by the etching time[26], although not linearly etched. The nanostructured $SiO_2$ surfaces in case of Ni deposition time for 60 s when the etching time was controlled to 15 min., the nanopillar height was approximately 234.30 nm. By extending the etching time to 30 min. and 45 min., the height was increased to 589.09 nm and 645.28 nm, respectively. Finally, when the etching time was increased to 60 min., the nanostructure height was approximately 667.60 nm. Furthermore, the height of nanopillars using Ni deposition time for 90 s were increased after etching time from 15 min. to 60 min. The height after 15, 30, 45 and 60 min. of etching were 255.30, 522.70, 602.12 and 738.80 nm, respectively as shown in the Figure 4(e)-4(h).

From the Figure 4(a), the etching time of 15 min. clearly showed the etched structures into the $SiO_2$ material. The structures were nanopillar in shape that were directly etched straight from the surface normal. Although the etching time was small, the structure was well-maintained. In addition, the height of the nanopillar was consistent across the whole area of the sample. Figure 4(b) showed the increase in the etched depth of the $SiO_2$ surface. From the physical observations, the etched structures were also nearly well-defined in comparison to Figure 4(a). However, from close observations, the etched structures, especially on the trenches, side walls, or the bottom of the etched surface, appeared slightly deformed. The deformation of the etched bottom surface was more pronounced as also appeared in Figure 4(c) and 4(d). From these figures, the formation of taper-shaped profile was exhibited due to during the etching, the Ni mask patterns can also be etched by reactive ion.[3] For the larger size of Ni deposition time for 90 s can resist surface during

plasma etching more than the small Ni nanoparticles. As mentioned, the nanostructured $SiO_2$ surfaces in Figure 4(e)-4(h) were slightly deformations of nanopillars when compared with nanostructured $SiO_2$ surfaces in case of Ni deposition time for 60 s.

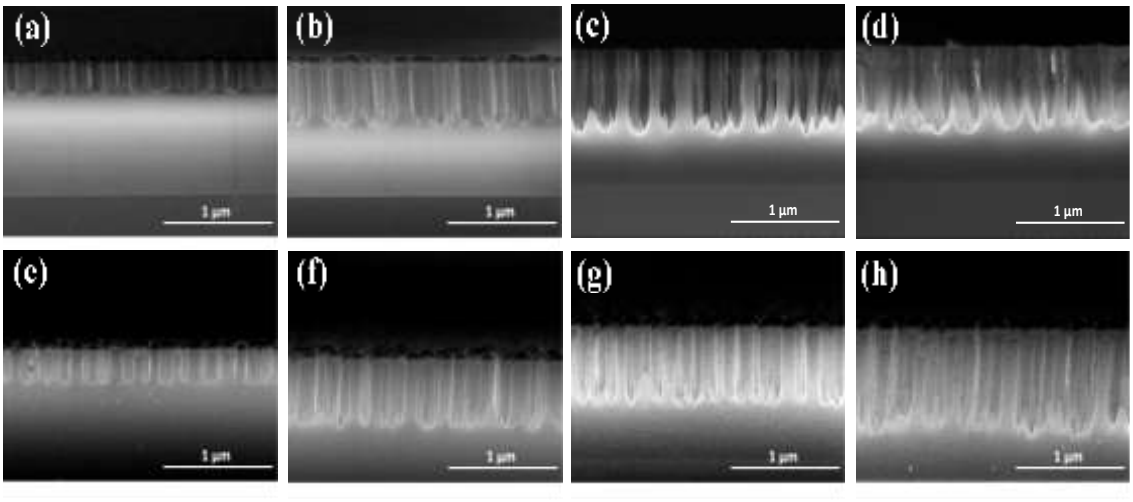


**Figure 4.** SEM images of nanostructured $SiO_2$ layers etched for (a) 15 min. (b) 30 min. (c) 45 min. (d) 60 min. (Ni deposition time for 60 s) (e) 15 min. (f) 30 min. (g) 45 min. and (h) 60 min. (Ni deposition time for 90 s)

*Effect of morphology of nanostructured surfaces with optical properties*

The optical properties were studies on $SiO_2$ nanostructure in terms of surface reflectance. The reflectance of the bare $SiO_2$ and nanostructured $SiO_2$ surfaces was measured by UV-VIS-NIR spectrophotometer.

Figure 5 shows the average reflectance measured as a function of the different etching time. The reflectance of bare $SiO_2$ is also presented for comparison. The average reflectance of bare $SiO_2$ was 25.24% in a spectral range from 380-750 nm. In case of Ni deposition time for 60 s, the sub wavelength structures at etching time 15 min. shows the average reflectance value of 4.30%. The reflectance of the structure is decreased as the height of the structure increases. However, the increasing of duration time affected deformations of $SiO_2$ nanostructure as a results the average reflectance is increased when duration time more than 15 min. The sample etched for 30, 45 and 60 min exhibited the average reflectance of 21.84%, 16.59% and 20.54%, respectively. For $SiO_2$ structure of Ni deposition time for 90 s. The $SiO_2$ nanostructure after etched for 15 and 30 min. shows the average reflectance value of 11.64% and 7.75% respectively. It can be seen that the average reflectance is decreased until the duration time was more than 30 min. As a results, the average reflectance of 17.76%, and 17.85% for etching time at 45 and 60 min., respectively. In comparison to Ni deposition time for 60 s, the drastically increase of average reflectance was noticeable at a longer time due to the larger size of Ni nanoparticles at deposited time for 90 s can resist surface during plasma etching.

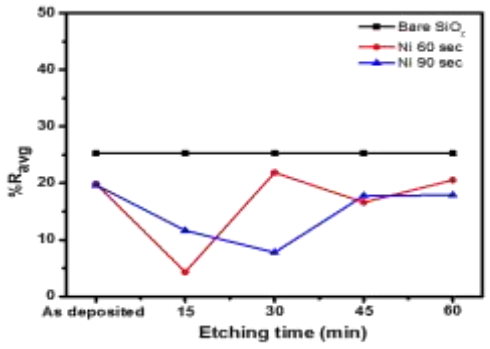


**Figure 5.** Optical reflectance of nanostructured $SiO_2$ surface measured as a function of plasma duration.

As mentioned before, the reflectance of the structure is expected to be decrease as the height of the structures increased were controlled by plasma etching duration. Moreover, the reflectance of the nanostructure surface did not depend only height of nanostructure, but also depend on the different average period.[4, 9] The reflectance tendency was related to a refractive index profile.[27-28] Therefore, to modify surface reflectance, the refractive index profile should be controlled.

## Conclusion

We have investigated the development of the nanostructured patterns based on the $CF_4$ plasma etching process on the $SiO_2$/Si substrates, in order to reduce surface reflection of materials. The nickel films were firstly deposited on the blank substrates at different deposition time. The samples were annealed in order to promote agglomeration into the Ni nanoparticles random patterns. The Ni nanoparticles prepared at different deposition times exhibited different average sizes in the diameter and then used as the metallic masks for the plasma etching process. After the $CF_4$ plasma etching, the final samples were thoroughly investigated by field-emission scanning electron microscopy (FESEM) and the UV-Vis-NIR spectroscopy to study the physical morphologies and optical transmission spectra for each sample condition. The results showed that the reflection characteristics could be controlled by plasma etching because of changing in morphology of nanostructured $SiO_2$ surfaces. The Ni deposition time of 60 s was to be used as the metallic masks after the annealing treatment. The plasma etching time was best performed at 15 minutes. The sample was exhibited smallest average reflectance value of 4.30%

## References

1. Raut, H.K., Ganesh Nair V.A. and Ramakrishna, A.S. S. (2011). Anti-Reflective Coatings: A Critical, In Depth Review. *Energy Environ. Sci.* **4**: 3779-3804.

2. Chattopadhyay, Huang S., Jen Y.F., Ganguly Y.J., A. Chen, K.H. Chen, L.C. (2010). Anti-Reflecting and Photonic Nanostructures. *Mater. Sci.Eng. R-Rep.* **69**: 1-35.

3. Ye, Jiang X., Huang X., Geng J., Sun F., Zu L., Wu X. and Zheng W., W. (2015). Formation of Broadband Antireflective and Super-hydrophilic Subwavelength Structures on Fused Silica Using One-Step Self-Masking Reactive Ion Etching. *Sci. Rep.* **5**: 13023.

4. Park, G.C., Song, Y.M., Ha, J-H. and Lee, Y.T. (2011). Broadband Antireflective Glasses with Subwavelength Structures Using Randomly Distributed Ag Nanoparticles. *J. Nanosci. Nanotechnol.* **11**: 6152-6156.

5. Shang, P., Xiong, S.M., Deng, Q.L., Shi, L.F. and Zhang, M. (2014). Disordered Anti reflective Subwavelength Structures Using Ag nanoparticles on Fused Silica Windows. *Appl. Opt*. **53(29)**: 6789-6796.

6. Ye, X., Huang, J., Geng, F., Sun, L., Hongjie, L., Jiang, X., Wu, W., Zu, X. and Zheng, W. (2016). Broadband Antireflection Sub-wavelength Structures on Fused Silica Using Lower Temperatures Normal Atmosphere Thermal Dewetted Au Nanopatterns. *IEEE Photon. Technol. Lett.* **8(1):** 2700110.

7. Xu, H., Lu, N., Qi, D., Hao, J., Gao, L., Zhang, B. and Chi, L. (2008). Biomimetic Antireflective Si Nanopillar Arrays. *Small.* **4(11):** 1972-1975.

8. Wang, S., Yu, X.Z. and Fan H.T., (2007). Simple Lithographic Approach for Subwavelength Structure Antireflection. *Appl. Phys. Lett.* **91:** 061105.

9. Lee, Y., Koh, K., Na, H., Kim, K., Kang J-J. and Kim, J. (2009). Lithography-Free Fabrication of Large Area Subwavelength Antireflection Structures Using Thermally Dewetted Pt/Pd Alloy Etch Mask. *Nanoscale Res. Lett.* **4(4):** 364-370.

10. Tulli, D., Hart, S.D., Mazumder, P., Carrilero, A., Tian, L., Koch, K.W., Yongsunthon, R., Piech, G.A. and Pruneri, V. (2014). Monolithically Integrated Micro- and Nanostructured Glass Surface with Antiglare, Antireflection, and Super-hydrophobic Properties. *Appl. Mater. Interfaces.* **6(14):** 11198-11203.

11. Lowdermilk, W.H., and Milam, D., (1980). Graded-Index Antireflection Surfaces for High-Power Laser Applications. *Appl. Phys. Lett.* **36:** 891-893.

12. Hedayati, M.K. and Elbahri, M. (2016). Antireflective Coatings: Conventional Stacking Layers and Ultrathin Plasmonic Metasurfaces, A Mini-Review. *Materials* **9(6):** 497.

13. Leem, J.W., Yeh, Y. and Yu, J.S. (2012). Enhanced transmittance and hydrophilicity of nanostructured glass substrates with antireflective properties using disordered gold nanopatterns. *Optics Express.* **20(4):** 4056

14. Lalanne, P. and Morris, G.M. (1996). Design, Fabrication and Characterization of Subwavelength Periodic Structures for Semiconductor Antireflection Coating in the Visible Domain. *Proc. SPIE.* **2776:** 300-309.

15. Walheim, S., Schäffer, E., Mlynek, J. and Steiner, U. (1999). Nanophase-Separated Polymer Films as High-Performance Antireflection Coatings. *Science.* **283:** 520-522.

16. Wang, S., Yu, X.Z. and Fan, H.T. (2007). Simple Lithographic Approach for Sub-wavelength Structure Antireflection. *Appl. Phys. Lett.* **91(6):** 061105.

17. Leem, J.W., Yu, J.S., Song, Y.M. and Lee Y.T. (2011). Antireflection Characteristics of Disordered GaAs Subwavelength Structures by Thermally Dewetted Au Nanoparticles. *Sol. Energy Mater. Sol. Cells.* **95(2):** 669-676.

18. Vitanov, P., Harizanova, A., Ivanova, T. and Dikov, H. (2014). Low-Temperature Depositionof Ultrathin SiO2 Films on Si Substrates. *J. Phys. Conf. Ser.* **514:** 012010.

19. Hiller, D., Zierold, R., Bachmann, J., Alexe, M., Yang, Y., Gerlach, J.W., Stesmans, A., Jivanescu, M., Müller, U., Vogt, J., Hilmer, H., Löper, P., Künle, M., Munnik, F., Nielsch, K. and Zacharias, M. (2010). Low Temperature Silicon Dioxide by Thermal Atomic Layer Deposition: Investigation of Material Properties. *J. Appl. Phys.* **107:** 064314.

20. Schaepkens, M., Oehrleina, G.S. and Cook, J.M. (2000). Effect of Radio Frequency Bias Power on $SiO_2$ Feature Etching in Inductively Coupled Fluorocarbon Plasmas. *J. Vac. Sci. Technol. B: Microelectron. Nanometer Struct. Process Meas. Phenom.* **18:** 848-855.

21. Son, J., Kundu, S., Verma, L.K., Sakhuja, M., Danner, A.J., Bhatia, C.S. and Yang, H. (2011). A Practical Superhydrohilic Self Cleaning and Antireflective Surface for Outdoor Photovoltaic Application. *Sol.Energ. Mat. Sol. Cells.* **98:** 46-51.

22. Verma L.K., Sakhuja M., Son, J., Danner A.J., Yang H., Zeng H.C and Bhatia C.S. (2012). Self-Cleaning and Antireflective Packaging Glass for Solar Modules. *Renew. Energy.* **36:** 2489-2493.

23. Thompson, C.V. (2012). Solid-State Dewetting of Thin Films. *Annu. Rev. Mater. Res.* **42:** 399-434.

24. Kim, D., Giermann, A.L. and Thompson, C.V. (2009). Solid-State Dewetting of Patterned Thin Films. *Appl. Phys. Lett.* **95(25):** 251903.

25. Park, G.C., Song, Y.M., Kang, E.K. and Lee, Y.T. (2012). Size-Dependent Optical Behavior of Disordered Nanostructures on Glass Substrates. *Appl. Opt.* **51(24):** 5890-5896.

26. Song, Y.M., Park, G.C., Kang, E.K., Yeo, C.L. and Lee, Y.T. (2013). Antireflective Grassy Surface on Glass Substrates with Self-Masked Dry Etching. *Nanoscale Res. Lett.* **8:** 505

27. Cho, S.J., An, T., Kim, J.Y., Sung, J. and Lim, G. (2011). Super hydrophobic Nano-structured Silicon Surfaces with Controllable Broadband Reflectance. *Chem. Commun.* **47(21):** 6108-6110.

28. Sakuma, S., Sugita, M. and Arai, F. (2013). Fabrication of Nanopillar Micropatterns by Hybrid Mask Lithography for Surface-Directed Liquid Flow. *Micromachines.* **4(2):** 232-242